ChemPubSoc Europe

DOI: 10.1002/cptc.201900235

CHEMPHOTOCHEM Articles

On the Aggregation Behaviour and Spectroscopic Properties of Alkylated and Annelated Boron-Dipyrromethene (BODIPY) Dyes in Aqueous Solution

Ana B. Descalzo,*[a, b] Pichandi Ashokkumar,[a, c] Zhen Shen,[d] and Knut Rurack*[a]

The tendency of boron-dipyrromethene (BODIPY) dyes to associate in water is well known, and usually a cause for inferior fluorescence properties. Synthetic efforts to chemically improve BODIPYs' water solubility and minimize this problem have been numerous in the past. However, a deeper understanding of the phenomena responsible for fluorescence quenching is still required. Commonly, the spectroscopic behaviour in aqueous media has been attributed to aggregate or excimer formation, with such works often centring on a single BODIPY family. Herein, we provide an integrating discussion including very diverse types of BODIPY dyes. Our studies revealed that even subtle structural changes can distinctly affect the association behaviour of the fluorophores in water, involving different photophysical processes. The palette of behaviour found ranges from unperturbed emission, to the formation of H or J aggregates and excimers, to the involvement of tightly bound, preformed excimers. These results are a first step to a more generalized understanding of spectroscopic properties *vs.* structure, facilitating future molecular design of BODIPYs, especially as probes for biological applications.

1. Introduction

Boron-dipyrromethene or BODIPY dyes have become very popular for fluorescence labeling, in imaging applications and for optical sensor development as well as more recently in photodynamic therapy and organic photovoltaics. Their synthetic versatility and outstanding spectroscopic properties, especially their remarkably intense emission which is tunable across a considerably broad spectral range, from the visible to the near infrared (NIR), are the major reasons for this success. Among other popular dyes such as fluoresceins, rhodamines and cyanines, the applications and investigations involving BODIPYs have grown disproportionately high over the last two decades (Figure 1) and the literature reporting the synthesis of new BODIPYs and a description of their optical and chemical properties in organic media is abundant.[1–17] However, rather few efforts have been devoted to the study of their properties in aqueous solutions.[18–28] This is surprising because on one hand the peculiarities of the application of BODIPYs in water are long since documented even by commercial suppliers[29] yet on the other hand many of the aspired applications such as fluorescence labeling or sensing essentially require operation in aqueous solution. The reason might be related to the fact that although they are intrinsically zwitterionic, BODIPYs have a rather hydrophobic character. The tendency to form dimers, oligomers or larger aggregates in aqueous media is thus potentially higher as for the net charged dye classes mentioned

[a] *Prof. A. B. Descalzo, Dr. P. Ashokkumar, Dr. K. Rurack*
Chemical and Optical Sensing Division
Bundesanstalt für Materialforschung und -prüfung (BAM)
Richard-Willstätter-Straße 11, 12489 Berlin (Germany)
E-mail: knut.rurack@bam.de
[b] *Prof. A. B. Descalzo*
Present address: Dpmt. Organic Chemistry, Faculty of Chemistry
Complutense University of Madrid (UCM)
Av. Complutense, s/n, 28040, Madrid (Spain)
E-mail: ab.descalzo@quim.ucm.es
[c] *Dr. P. Ashokkumar*
Present address: Laboratoire de Bioimagerie et Pathologies, UMR 7021 CNRS
Faculté de Pharmacie, Université de Strasbourg
Strasbourg CS 60024 (France)
[d] *Prof. Z. Shen*
State Key Laboratory of Coordination Chemistry
Nanjing National Laboratory of Microstructures and
School of Chemistry and Chemical Engineering
Nanjing University
Nanjing 210046 (China)

Supporting information for this article is available on the WWW under https://doi.org/10.1002/cptc.201900235

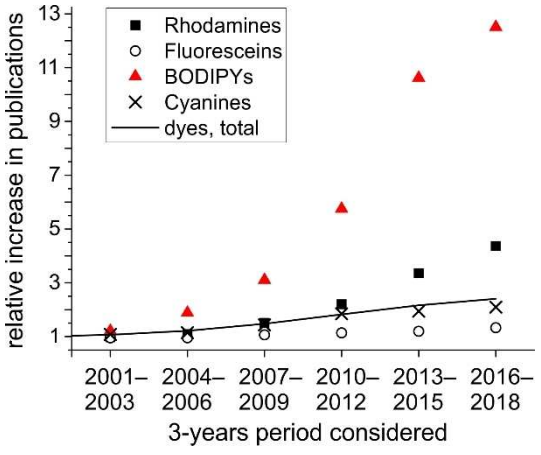

Figure 1. Increase in publications involving the dye families indicated (symbols) as well as dyes as such (trend line) in the respective periods relative to the period 1998–2000 (Web of Science, Clarivate Analytics).[30]

above; cationic rhodamines and cyanines, and anionic fluoresceins.

If common BODIPYs are used in water, the main consequences are usually a broadening and/or spectral shift of the absorption and emission bands and a strong diminution of the fluorescence, yielding solutions which are only poorly or virtually non-fluorescent. In contrast, if the dyes are well dissolved in water, the favorable absorption and fluorescence features observed for the dye in an organic solvent are retained. Especially problematic is the case of NIR-emitting BODIPYs since these chromophores tend to have larger aromatic structures and are thus more hydrophobic.[7,31] Several strategies have been reported to improve the water solubility of BODIPY dyes[8] such as the introduction of ionizable functional groups – carboxylate, sulfonate[18,32,33] or ammonium[33,34] groups – or the functionalization with carbohydrates,[35,36] dendrimers,[37,38] poly(ethylene glycol) (PEG) chains[18,21,24,39] or combinations thereof.[40,41] PEG functionalization can be even employed for NIR-emitting BODIPYs.[19,22,23,33,42,43] Alternatively, it is also possible to obtain highly fluorescent objects with hydrophobic BODIPY dyes in aqueous media if they are encapsulated in polymeric nanoparticles.[44] Ziessel et al. have recently performed an interesting comparative study of the ability of different hydrophilic groups to improve water solubility for a series of BODIPYs and derived a water-solubility scale by determining the partition coefficient and fluorescence quantum yield for each polar BODIPY dye.[24] Introduction of bulky substituents into the fluorophore core is also a strategy for decreasing aggregation-induced quenching when poorly dissolving solvents are employed. For example, a recent work reports the derivatization of BODIPY dyes with tetraphenylethene moieties.[45] These derivatives form highly emissive aggregates in THF:water mixtures when the percentage of water is $\geq$80%.

Based on our experience in the field of BODIPY dyes and their spectroscopic properties[44,46–49] and due to the fact that we also encountered diverse behaviour of these dyes in water during various investigations,[50,51] we embarked on a study of the spectroscopic properties of a series of BODIPYs in aqueous media. As will be detailed below, different spectroscopic patterns can be expected for BODIPYs in aqueous environments. While these observations have been attributed to various types of dimers or aggregates in the past, it is remarkable to note that only two slightly different BODIPY cores have been involved in these previous studies (Scheme 1). In addition, the studies either utilized some kind of chemical confinement, mostly with biomolecular superstructures, or aggregate-promoting long-chain substituents to probe BODIPY structure diversity. To get a better fundamental understanding, we opted for a more systematic study by employing a series of structurally differentiated BODIPYs and by excluding any chemically interacting environment such as micelles, skeleton backbones or protein pockets. As alluded to above, this is especially important for dyes which absorb and emit at longer wavelengths than those shown in Scheme 1. In addition, precipitation and re-dissolution issues due to the presence (or as a function of the concentration) of solubilizing entities such as vesicles or biomacromolecules can lead to severe errors in intensity-based measurements. For our study, we employed several rather simple BODIPYs (**R$_x$BDP-Y**), a benzene-fused BODIPY (**BBDP-Ph**), a series of dihydronaphthalene-fused BODIPYs (**DHNBDP-H**, **DHNBDP-Me**, **DHNBDP-Ph**) and three phenanthrene-fused dyes (**PBDP-Ph**, **PBDP-DMA**, **PBDP-CN**), carrying chemical groups with distinctly different electron donating or accepting character in the *para*-position of the *meso*-substituent (Scheme 2). Most of these derivatives are highly fluorescent in organic solvents, and especially interesting are the **BBDP**,[47] **DHNBDP**[48] and **PBDP**[44,49] dyes, because they show a strong fluorescence in the red-NIR spectral region.

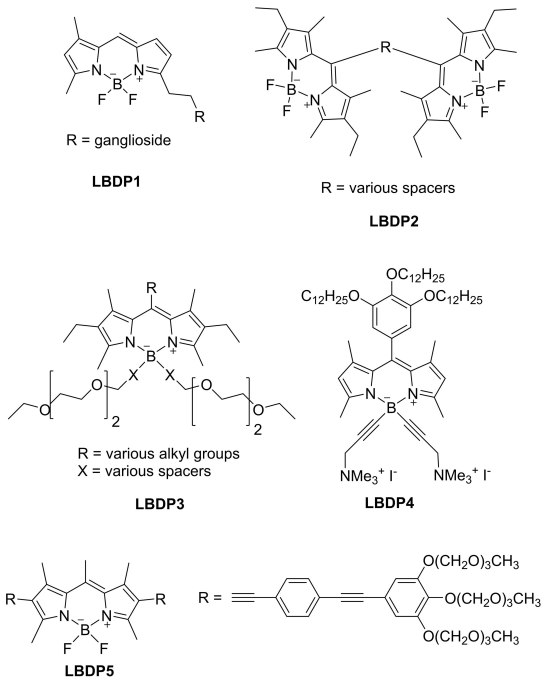

Scheme 1. BODIPYs investigated in water in previous literature studies.

1.1. Previous Observations on Association

Before we present our results, it is helpful to reflect the current state of knowledge on BODIPY association in water. BODIPYs can aggregate in different ways. For example, in one of the first works on BODIPY dimers, the authors observed the formation of two different kinds of ground state dimers, which were formed under different experimental conditions, so-called D_I and D_{II} dimers (for dye structure, see Scheme 1).[52] D_I dimers were observed when two **LBDP1** dyes were forced to be in adjacent position by covalently linking them to a protein. D_{II} dimers appeared when the same BODIPY cores were encapsulated in lipid phases (micelles or vesicles). D_I dimers were non-fluorescent and possessed a blue-shifted absorption with respect to the monomer band. The structure of the protein was assumed to allow two **LBDP1** to be at distances short enough for the molecular planes to become parallel, entailing efficient orbital contact. In the lipid systems, D_I dimers were found to

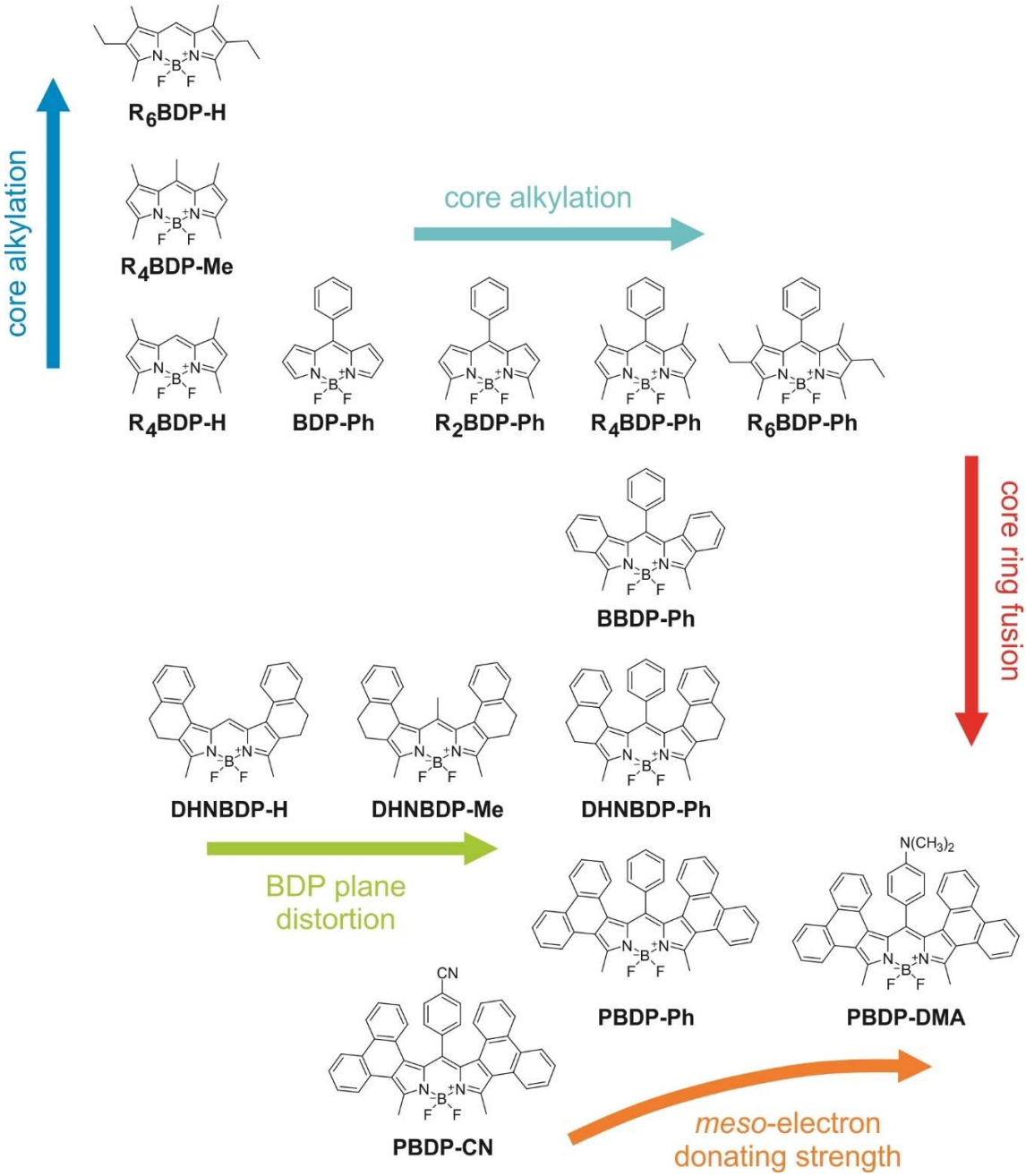

Scheme 2. Chemical structures of the BODIPYs investigated, arranged according to increasing core alkylation (blue and blue-green arrows), degree of fusion of additional π systems to the main BODIPY core (red arrow), increasing distortion of the BODIPY three-membered ring plane (green arrow) and an increasing electron-donating strength of the substituent in the *meso*-position (orange arrow).

co-exist with the D_{II} dimers featuring a new red-shifted absorption band. Upon excitation, an emission band centered at ca. 630 nm was thus observed, red-shifted with respect to the emission of the monomer (at ca. 515 nm). From exciton theory, the authors concluded that the higher-energy transition observed for D_I dimers corresponds to the planes of two BODIPY moieties stacking upon each other so that the electronic transition dipoles are preferentially parallel. On the other hand, the band at lower transition energy observed for D_{II} dimers was attributed to the molecular planes of **LBDP1** being located within the same plane with preferentially collinear transition dipoles.

In a related work, the same authors discarded excimer formation to be the cause for the emission of the D_{II} dimers at 630 nm on the basis of fluorescence anisotropy measurements.[53] In another work, Brennan et al. reported the use of molecular confinement within a sodium silicate-derived glass system in which non-fluorescent BODIPY H dimers of **R_4BDP-H** (Scheme 2) can be formed, without any interference from higher-order aggregates or fluorescent J dimers.[54] The fluorescence quantum yield of the H dimer was found to be

close to zero. The authors also described the dimerization of **R_4BDP-H** in aqueous solution. By performing absorption studies as a function of time, they observed that in solution the dimerization presumably proceeded slowly via a non-fluorescent aggregate, possibly involving precipitation, because the bands in the absorption spectrum only decreased non-specifically over 24 h. After several days, a new blue-shifted absorption band appeared which was then attributed to the H dimer according to exciton theory. Besides ground-state dimerization and different species serving as intermediates, Howgego et al. put forward the possibility of excimer formation via prearranged and fixed dimers.[55] The authors prepared covalently linked, symmetrical dimers of **LBDP2** (Scheme 1), connected via different linkers that provide co-facial arrangement of two BODIPYs with different bite angles between the planes of the chromophore units, resulting in different overlap of the chromophores and different electronic interactions.[56] They observed that only the compound with the smallest bite angle showed excimer emission in solution under ambient conditions. Other authors have also observed that BODIPY dyes of **LBDP1** type can show excimer fluorescence at high local concentrations when performing studies in membranes.[57–59]

Chujo et al. studied the aggregation behaviour of a series of amphiphilic **LBDP3** dyes (with different PEG substituents) in mixtures of THF:water.[20] One of these BODIPYs showed aggregates derived from H dimers, forming spherical nanoparticles in aqueous THF (with a diameter of 3.9 ± 0.6 nm, assembling into larger aggregates of ca. 100 nm as shown by TEM images and DLS measurements). Studies carried out in THF and THF:water mixtures ($c_{dye} = 10$ μM) revealed that an increase of the water ratio was related to a decrease of the molar absorption coefficient. An isosbestic point at 480 nm was observed for one of the dyes, attributed to the two-state equilibrium in which H dimers grow at the expense of monomers as the water content is increased. On the other hand, Ziessel et al. reported NIR fluorescent nanoparticles formed by the J aggregation of hydrophobic BODIPY dyes in THF:water mixtures.[60] Aggregation studies of positively charged (**LBDP4**) and net neutral (**LBDP5**) long chain-substituted amphiphilic BODIPYs in water yielded the formation of H- and/or J-type aggregates.[25,26,28] Temperature- and concentration-dependent UV/Vis studies revealed that aggregation of **LBDP4** occurs via a cooperative process, resulting in vesicles with a multilamellar wall structure.[25] In the case of **LBDP5**, only H aggregates were observed, this time leading to spherical nanoparticles by non-cooperative self-assembly.[26] These reports necessitate a more comprehensive understanding of aggregation of various types BODIPY dyes in aqueous media.

2. Results and Discussion

2.1. Absorption and Fluorescence Properties

The solvatochromism and/or solvatokinetics of most of the compounds investigated here (Scheme 2) in organic solvents have been studied earlier by others and us[46–49] and the relevant data are included in the Supporting Information of this paper for better comparison (Table S1). In organic solvents, most of the compounds show moderate to strong fluorescence ($\Phi_f = 0.4$–1.0), except for the compounds having flexible *meso*-phenyl groups (**BDP-Ph**; $\Phi_f \approx 0.02$ and **R_2BDP-Ph**; $\Phi_f = 0.17$–0.33) or a donor-acceptor substitution pattern (**PBDP-DMA** in polar solvents; $\Phi_f \approx 0.025$). Accordingly, k_r and k_{nr} values are also similar for all compounds in organic solvents with the above noted exceptions (see Table S1 in the Supporting Information). However, in water most of the compounds show a diverse spectroscopic behaviour, depending on their chemical structure which has been investigated in a systematic manner here. The studies described in this manuscript have been performed with 1 μM and 5 μM solutions of the corresponding BODIPY dye in (i) 100% acetonitrile (MeCN, as a reference of a neat organic medium) and (ii) water with 2.5% (*v/v*) MeCN; this small percentage of MeCN corresponds to the small amount of an acetonitrile stock solution that had to be employed for the studies in water to circumvent any dissolution errors when trying to prepare stock solutions directly in water and was kept constant in all the experiments. In the following, these two types of solutions will be referred to as "organic" and "aqueous".

2.2. Influence of Solvent Composition in Mixed Organo-Aqueous Solvents

Before embarking on a comparative study of the dyes in the two different solvents and because we had to employ a residual amount of acetonitrile from the stock solutions in our experiments, it is important to assess whether this quantity can influence the outcomes. We thus studied the behaviour of a representative dye of each class (see below for details) in acetonitrile-water mixtures of varying compositions. As Figure 2 shows by the example of **PBDP-Ph**, a dramatic change in the spectroscopic properties occurs when the fraction of water exceeds 60%. Moreover, this change happens in a considerably small percentage range of water (see inset of Figure 2) and can be witnessed in parallel in both, absorption and emission spectra. A similar behaviour was found for **DHNBDP-Me** (also above 60% of water), for **R_4BDP-Me** and **R_6BDP-Ph** (above 70%) and for **R_4BDP-Ph** (above 80%). **BBDP-Ph** showed gradual

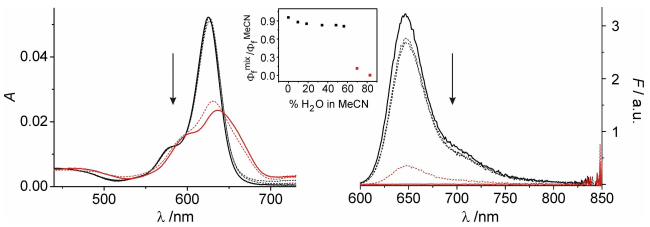

Figure 2. Absorption (left) and emission ($\lambda_{ex} = 595$ nm) for **PBDP-Ph** in MeCN (black) and in mixtures of MeCN:H_2O; water content: 48 and 56% (dashed black), 70% (dashed red) and 83% (red). Inset: Variation of the fluorescence quantum yield (Φ_f) of **PBDP-Ph** as a function of % H_2O in MeCN. The concentration of the dye was kept constant at 2 μM in all cases.

and time-dependent changes already at low water ratios of ca. 20%, with massive spectral changes of the longest-wavelength band also occurring at >80% of water. Only **R_4BDP-H** did not show any significant variation over the entire range of solvent compositions (for comprehensive data, see Figures S1–S5).

2.3. Influence of Dye Concentration

In the case of organic solutions, identical spectroscopic characteristics are shown by the 1 and 5 μM samples. The only difference found was a small red-shift of the emission maximum (1–2 nm) for the more concentrated solutions (c = 5 μM), which is due to re-absorption effects for dyes with such small Stokes shifts in solutions with absorbances ⩾0.1; this effect is absent when recording the fluorescence in 1 mm cells and a front-face geometry. In the case of aqueous solutions, increasing dye concentration from 1 to 5 μM has, in some cases, additional effects, such as a change in the shape of the absorption spectrum and deactivation of the fluorescence or formation of a new fluorescence band. The last will be discussed in more detail in the next sections.

From the series displayed in Scheme 2, we can classify the dyes according to their behaviour in aqueous vs. organic medium as follows: (i) Dyes whose optical properties remain almost unaltered when changing the medium from organic to aqueous, and also when increasing the dye concentration in both solvents from 1 μM to 5 μM (except for the re-absorption phenomenon discussed above). Here, **R_4BDP-H** and **BDP-Ph** belong to this class. (ii) Dyes that display strong changes in the absorption spectrum in water: a dramatic broadening together with a hypso- or bathochromic shift with respect to the band in organic solution; this behaviour is typically stronger at elevated dye concentration. In conjunction with these spectral shifts, an offset of the absorption spectra can often be noticed (in particular after tens of minutes or longer times) indicating that larger, more insoluble aggregates (or non-specific precipitates) are formed that increase the scattering intensity of the solution, producing a decrease in transmission. As discussed in the literature, it is expected that H aggregates would result in the appearance of blue-shifted absorption bands, together with a dramatic quenching of the emission, while J aggregates would give rise to a red-shifted absorption band. Excitation in this red-shifted band should ideally yield a narrow, almost resonant fluorescence. Among the dyes investigated, **R_4BDP-Me** shows an H aggregate-like behaviour while **R_2BDP-Ph** and **R_4BDP-Ph** resemble the behaviour expected for J aggregates. (iii) An intermediate case are **R_6BDP-H** and **R_6BDP-Ph** that do not display a shift in their absorption maxima, but a pronounced decrease of the absorption coefficient (ε) and a quenching of the fluorescence in aqueous samples. It is important to note that within class (i) to (iii) all the dyes consist of the minimal dipyrrin core and differ only in their alkyl or phenyl substitution pattern at the core. When stepping on to more deeply absorbing and emitting dyes by core-fusion of aromatic π-systems—benzene, dihydronaphthalene or phenanthrene, their chemical nature becomes more hydrophobic yet still these dyes differ in behaviour. Class (iv) shows changes in the vibronic structure of the absorption band in aqueous solution compared with the organic counterpart yet largely unaltered emission bands. The latter are only slightly red-shifted by 3–4 nm with respect to the emission of the dye in MeCN and reflect the characteristics of BODIPY (locally excited or LE) monomer emission (**BBDP-Ph**). Class (v) and (vi) dyes finally display only a very weak or virtually no LE emission, but a broad, structure-less and red-shifted new emission band in the NIR region (**DHNBDP-H**, **DHNBDP-Me**, **DHNBDP-Ph**, **PBDP-Ph**, **PBDP-DMA** and **PBDP-CN**).

2.4. Dipyrrin BODIPYs

2.4.1. Class (i): BODIPYs with Good Water Solubility

For **R_4BDP-H** and **BDP-Ph**, the spectral properties in an organic solvent and in aqueous solution are almost identical (Table 1). Figure 3 shows the normalized absorption, fluorescence emission and excitation spectra in water and MeCN at c = 5 μM for the two dyes. Because of its flexible nature being able to adopt a non-emissive butterfly-like conformation in the excited state, the fluorescence of **BDP-Ph**, the least substituted molecule in the series studied here, is distinctly lower than for all the other dyes also in the organic solvent as observed by its more than 100-fold higher k_{nr} value when compared to **R_4BDP-H** (Table S1).[61]

2.4.2. Class (ii): BODIPYs Prone to Aggregation

One of the most dramatic effects observed in the absorption spectra when changing the solvent from organic to aqueous is that observed for **R_4BDP-Me**, **R_2BDP-Ph** and **R_4BDP-Ph**. These changes are a function of the dye concentration and of the time as, apparently, aggregates are forming slowly in solution. Besides a broadening of the absorption spectra, in the case of the more concentrated aqueous solutions of the dyes there are dramatic differences between the absorption and fluorescence excitation spectra (Figures 4 and 5), indicating the existence of non-emissive species.

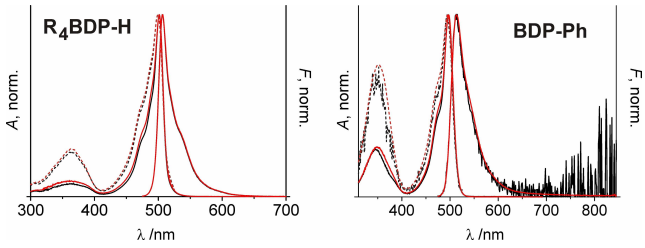

Figure 3. Normalized absorption and emission spectra in MeCN (black) and water (red) at c = 5 μM (λ_{ex} = 470 nm) for **R_4BDP-H** (left) and **BDP-Ph** (right); excitation spectra (dotted, uncorrected) in MeCN (black) and water (red) are shown for comparison.

Table 1. Spectroscopic properties of BODIPY dyes (except for those that show strongly time-dependent behaviour) in organic and aqueous solution at 1 μM and 5 μM at 298 K.

Dye	c [μM]	λ_{abs} [nm] (ε [10^4 M^{-1} cm^{-1}])		λ_{em} [nm]		τ_f [ns]	
		MeCN	H_2O	MeCN	H_2O	MeCN	H_2O
R_4BDP-H	1	501 (7.3)	501 (6.1)	506	506	5.28	5.81
	5	501 (7.3)	501 (6.4)	507	507	5.42	5.80
R_6BDP-H	1	526 (6.4)	526 (3.5)	534	534	5.62	6.07
	5	526 (6.3)	527 (2.9)	534	535	5.81	6.14
BDP-Ph	1	497 (5.1)	497 (4.8)	512	512	0.15	0.20
	5	497 (5.1)	497 (4.8)	513	513	0.14	0.19
R_6BDP-Ph	1	522 (6.8)	524 (3.4)	533	536	5.25	4.41
	5	522 (6.8)	524 (3.2)	535	536	5.22	4.39
BBDP-Ph	1	597 (11.8)	607 (2.5)	604	608	5.63	n.d.[a]
	5	597 (11.6)	608 (2.4)	607	608	5.74	0.15, 5.10[b]
DHNBDP-H	1	558 (7.9)	518 (2.3)	564	567 (w)/772	3.37	n.d.[a]
	5	558 (7.9)	517 (2.3)	566	567 (w)/772	3.32	[c]
DHNBDP-Me	1	559 (6.4)	565 (2.9)	596	none[d]/713	3.18	n.d.[a]
	5	559 (6.6)	565 (2.9)	597	none[d]/713	3.15	[c]
DHNBDP-Ph	1	565 (5.8)	550 (3.2)/582 (2.8)	611	none[d]/720	1.30	n.d.[a]
	5	565 (5.5)	550 (3.1)/582 (2.7)	611	none[d]/720	1.32	[c]
PBDP-Ph	1	627 (4.1)	639 (1.5)	646	none[d]/811	5.95	n.d.[a]
	5	627 (4.0)	639 (1.8)	648	none[d]/811	5.91	n.d.[a]
PBDP-DMA	1	617 (3.4)	624 (1.2)	623/801	666/778	[c]	n.d.[a]
	5	617 (3.8)	624 (1.2)	623/801	666/778	[c]	n.d.[a]
PBDP-CN	1	637 (5.6)	648 (2.2)	663	701/846	5.98	n.d.[a]
	5	637 (5.6)	648 (2.2)	663	701/846	5.91	n.d.[a]

[a] Not determined because of too low intensity or lying outside of the detection range of the time-resolved setup. [b] Biexponential decay with relative amplitudes of 0.48 (for 0.15 ns) and 0.52 (for 5.10 ns). [c] For details, refer to the corresponding sections below. [d] "None" refers to the absence of an appreciable emission band in the wavelength region of the typical BODIPY fluorescence resulting from BODIPY-core-localized excitation (LE emission).

Figure 4 shows the variation of the absorption spectra for **R_4BDP-Me** in aqueous solution when gradually increasing the concentration of the dye in the cuvette from 1 to 16 μM. Besides a strong broadening of the band, an increase in background signal (offset) is observed, indicating the formation of particulate objects which produce enhanced scattering.[62] The formation of the aggregates is not only a function of the concentration, but also of the time. For instance, after 30 min further changes in the absorption features take place as illustrated by the 16 μM solution in Figure 4. From the overlay of absorption and fluorescence excitation spectra in Figure 4 (right) and the similar lifetimes observed in both MeCN (5.53 ns) and water (5.42 ns) for 5 μM solution it can be concluded that most of the aggregates formed are virtually non-fluorescent. The dramatic effect that the simple introduction of a methyl group at the *meso*-position (**R_4BDP-Me** vs. **R_4BDP-H**) exerts on the solubility properties of the dye in aqueous environments is remarkable. The fact that the absorption of the aggregates is mainly blue-shifted with respect to the absorption of the monomer and that the aggregates are virtually non-fluorescent strongly suggests the formation of H-aggregates for **R_4BDP-Me** in water.

The behaviour of **R_2BDP-Ph** and **R_4BDP-Ph** in aqueous samples resembles that of **R_4BDP-Me**: a broadening of the absorption spectra upon increasing dye concentration and as a function of time (Figure 5). In this case, however, a red-shifted band appears at 535 nm for **R_4BDP-Ph** at 5 μM. The full width at half maximum (FWHM) of this band amounts to only 350 cm^{-1} which is still distinctly narrower than the bands of rigid and planar BODIPYs such as **BBDP-Ph** (ca. 550 cm^{-1}, see Ref. [47]). When exciting at this red-shifted band, a new, very narrow emission band (fwhm = 240 cm^{-1}) can be observed at

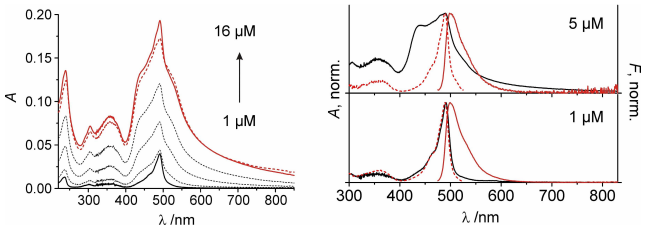

Figure 4. Left: Absorption of **R_4BDP-Me** in aqueous solution at different concentrations between 1 (black) and 16 μM (red, solid at $t = 0$, dotted at $t = 30$ min), steps of 2, 5, 10 μM. Right: normalized absorption (black), emission (red, $\lambda_{ex} = 470$ nm) and excitation spectra (dotted, $\lambda_{em} = 530$ nm) for 1 μM (bottom) and 5 μM (top) aqueous solutions of **R_4BDP-Me**.

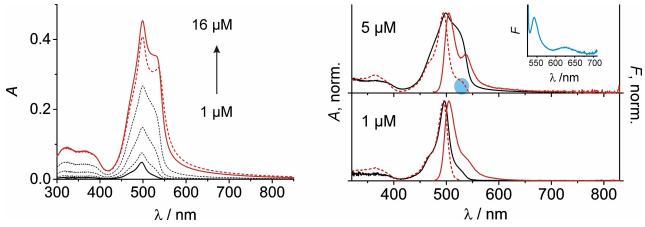

Figure 5. Left: Absorption of **R_4BDP-Ph** in aqueous solution at different concentrations between 1 (black) and 16 μM (red, solid at $t = 0$, dotted at $t = 10$ min), steps of 2, 5, 10 μM. Right: Normalized absorption (black), emission (red, $\lambda_{ex} = 470$ nm) and excitation spectra (dotted, $\lambda_{em} = 530$ nm for 1 μM and $\lambda_{em} = 555$ nm for 5 μM) for 1 μM (bottom) and 5 μM (top) aqueous solutions of **R_4BDP-Ph**; blue area highlights red-absorbing fluorescent species. The inset shows the emission of 5 μM **R_4BDP-Ph** in water upon excitation at 524 nm.

543 nm. **R_2BDP-Ph** requires higher concentration (>10 μM) to yield a similar behaviour as **R_4BDP-Ph** (Figure 6). These facts seem to indicate the formation of J aggregates. Apparently, **R_2BDP-Ph** and **R_4BDP-Ph** present a different aggregation pattern than **R_4BDP-Me**, most probably due to the presence of the orthogonally twisted phenyl substituent in the *meso*-position. The latter seems to disfavor a stacking-like arrangement of dye monomers at the expense of a more in-plane arrangement with preferential head-to-tail collinear transition dipoles. If we compare the magnitude of the J-bands with classical J-aggregate forming dyes such as cyanines, it is obvious that the amount of dye molecules forming the aggregates is much less in number and hence their order is lower. Exciton delocalization lengths of >10 molecules as seen for cyanines are most likely not reached here.[63,64] As has been recently shown by Werz's group, chemical fixation of BODIPY units to oligomers can strongly drive J aggregate formation.[65] These authors have also observed that subtle structural modifications can have a pronounced impact on the nature of the aggregates formed.

2.4.3. Class (iii): BODIPYs with Low Water Solubility

Regarding this class, again the influence of minor modifications in the chemical structure of a BODIPY dye on its spectroscopically manifested aggregation pattern is remarkable. **R_6BDP-H** and **R_6BDP-Ph**, which are structurally closely related to **R_4BDP-H** and **R_4BDP-Ph** and only differ in the two ethyl substituents that have been introduced in the 2- and 6-positions, show also a broadening of the absorption spectrum in water, more pronounced for the bulkier **R_6BDP-Ph** compared to **R_6BDP-H**, accompanied by a decrease in ε at the absorption maximum when going from the organic to the aqueous solution (Figure 7, Table 1). Moreover, a distinct decrease of the emission intensity is noticed especially for **R_6BDP-Ph** (>10× with respect to an organic solution of similar concentration, s. Figure S5). The latter however is basically due to the changes in absorption as the reduction in fluorescence for solutions having similar absorbance is only 1.2-fold in aqueous compared with organic solvents, which is well reflected in the only 1.2-fold reduced fluorescence lifetime in water (Table 1). Comparing absorption and fluorescence excitation spectra of **R_6BDP-Ph** in organic and aqueous solution it is obvious that the broadening is much less pronounced than for the class (ii) dyes (Figure S7). We thus tentatively ascribe the behaviour of **R_6BDP-Ph** to a significant proportion of the molecules forming either non-fluorescent dimers or existing in a conformation that does not show sizeable fluorescence upon excitation. **R_6BDP-H** behaves qualitatively similar.

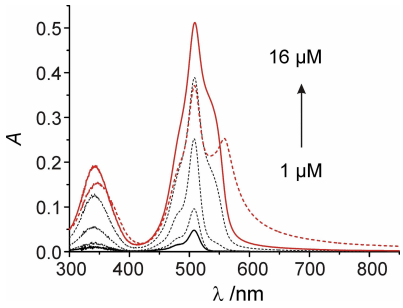

Figure 6. Absorption of **R_2BDP-Ph** in aqueous solution at different concentrations between 1 (black) and 16 μM (red, solid at $t=0$, dotted at $t=10$ min), steps of 2, 5, 10 μM. A new narrow red-shifted band is found at 559 nm for 16 μM solution at $t=10$ min. A representative 3D fluorescence plot is shown in Figure S6.

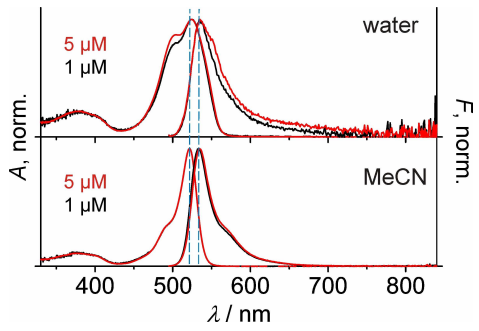

Figure 7. Absorption and emission (normalized) for **R_6BDP-Ph** in organic (bottom) and aqueous (top) solution at 1 μM (black) and 5 μM (red) ($\lambda_{ex}=490$ nm).

2.5. Aromatic Ring-Fused BODIPYs

The dyes containing an aromatic π-system fused to the BODIPY core present also a broadening of the absorption band in water. However, the shape of the spectrum does not depend on concentration (in the concentration interval considered here). Another more striking feature of this class of compounds is that the fluorescence intensity is even more dramatically quenched in aqueous solution than for classes (ii) and (iii). Moreover, in most cases, a new broad and red-shifted emission band appears, yet the fluorescence excitation and absorption spectra show perfect overlap.

2.5.1. Class (iv): Conformationally Reconfigured BODIPYs

In the case of **BBDP-Ph**, ε decreases more than 4 times in aqueous solution at 607 nm, but when integrating the entire absorption band corresponding to the $S_1 \leftarrow S_0$ transition after conversion to the energy scale (from ca. 13730 to 20470 cm^{-1}), only a ca. 1.4-fold decrease is found for the aqueous *vs.* organic medium; qualitatively, **BBDP-Ph** resembles class (iii) only with much stronger characteristics. Moreover, the most pronounced features described for the aggregating dyes above have not been found for **BBDP-Ph**. Regarding fluorescence, the emission is strongly quenched by more than 100× for 1 μM solutions and even further decreased when increasing the concentration in aqueous media. The position and the shape of the emission bands, however, remain rather constant in both solvents, yet consideration of the fluorescence excitation spectra in aqueous solution reveals a pronounced mismatch with the absorption

spectra (Figure 8). The absence of concentration- and time-dependent changes (below 80% of water) in the absorption spectra, the only slight change in integral absorption between 490–720 nm and the mismatch between absorption and excitation spectra suggest that the co-existence of different ground-state conformers in solution, which cannot interconvert during the lifetime of the excited state and among one of which is only significantly fluorescent, is the most probable scenario for **BBDP-Ph**. This assumption is supported by fluorescence lifetime data and fluorescence excitation spectra as a function of the emission wavelength. For instance, biexponential decays (Table 1), a long lifetime component of 5.10 ns (similar to the one observed in MeCN) and a new short component of 0.15 ns, are found across the narrow emission band with an almost 1:1 ratio of the two species involved and no significant dependence of the amplitude ratio on emission wavelength. In addition, observation of the fluorescence excitation spectra across the emission spectrum between 615 and 670 nm yields identical excitation spectra. Although this dye is known to possess an orthogonal conformation with respect to *meso*-substituent and BODIPY core,[47] the occurrence of propeller-like conformations has been found for other ring-fused BODIPYs.[44,48,49] Induction of such a structural change in a highly polar solvent such as water would thus not be unexpected. Moreover, as has been detailed in Ref. [48], the absorption maxima of conformationally rather differently twisted BODIPYs are only shifted by a few nanometers (at most) and the different conformers show virtually identical dipole moments. The presence of two conformers only differing in an internal twisting of the *meso*-substituent with respect to the BODIPY plane and a certain twisting within the rigid plane itself would most likely not entail pronounced spectral shifts. The considerably narrow and monomer-like shape of the absorption spectra and the similarity of the excitation spectra do not hint at the formation of aggregates with sizeable species diversity.

2.5.2. Class (v): BODIPYs Undergoing Excimer Formation

This behavioural class of BODIPY dyes comprises the dihydronaphthalene-appended dyes **DHNBDP-H**, **DHNBDP-Me** and **DHNBDP-Ph**. In the case of the **DHNBDPs**, a similar situation as for **BBDP-Ph** is found. Whereas $\varepsilon_{\lambda max}$ decreases 3.4-times for **DHNBDP-H**, 2.2-times for **DHNBDP-Me** and 1.8-times for **DHNBDP-Ph** in aqueous solution, the reduction of the integral $S_1 \leftarrow S_0$ transition amounts to only 1.2-times for the three dyes. In addition, the influence of concentration on the shape of the absorption spectra in aqueous solution is insignificant (Figure 9). In the case of **DHNBDP-Me**, we tested a series of concentrations, see Figure 10, confirming the previous observations of an unchanged spectral shape. The main difference with respect to **BBDP-Ph** occurs in emission and excitation spectra (Figures 10, 11, S8). In the present series, the typical BODIPY-centered LE emission is only weak or virtually absent and an additional broad, strongly red-shifted and weakly fluorescent band is observed. As can be deduced from Figure 11, measurement of the fluorescence excitation spectrum as a function of observation wavelength across the emission range from ca. 600–850 nm yields a single excitation band only, which additionally matches the absorption spectrum within the experimental uncertainty. Figures 10 and 11 also show that the ratio

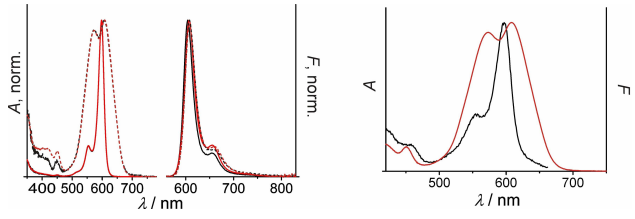

Figure 8. Left: Normalized absorption and emission spectra of **BBDP-Ph** in MeCN (solid line) and water (dotted line) at two different concentrations, 1 μM (black) and 5 μM (red). Right: Normalized absorption (red) and excitation (black, λ_{em} = 670 nm) spectra for **BBDP-Ph** in water at 5 μM.

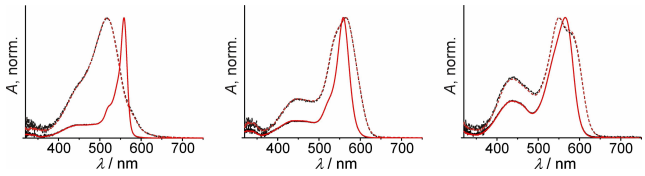

Figure 9. Normalized absorption spectra of **DHNBDP-H**, **DHNBDP-Me** and **DHNBDP-Ph** in organic (solid line) and aqueous medium (dotted line) at c = 1 μM (black) and 5 μM (red).

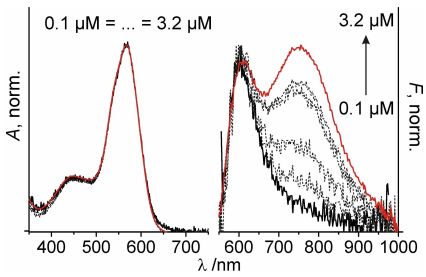

Figure 10. Normalized absorption and fluorescence spectra (λ_{ex} = 520 nm) of aqueous solutions of **DHNBDP-Me** at different concentrations from 0.1 μM (solid black) to 3.2 μM (red) with steps of 0.2, 0.4, 0.8 and 1.6 μM.

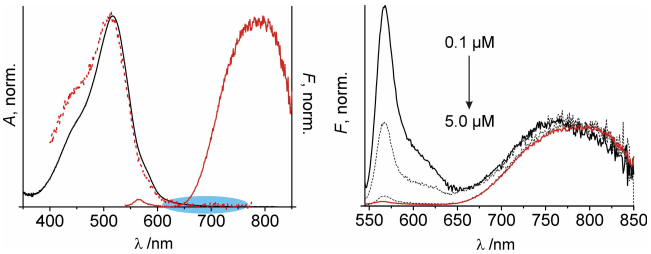

Figure 11. Left: Absorption (black), emission (red, λ_{ex} = 530 nm) and excitation spectrum (dotted, λ_{em} = 780 nm) of **DHNBDP-H** in water at 5 μM; blue area highlights absence of any red-absorbing fluorescent species. Right: Emission spectra (normalized to 1 at the red emitting band, λ_{ex} = 530 nm) for aqueous solutions of **DHNBDP-H** at different concentrations from 0.1 μM (solid black) to 5 μM (red) with steps of 0.2 and 1 μM.

between the LE and the red-shifted band depends on dye concentration in aqueous solution; the higher the concentration of the dye is the larger is the red-to-LE band ratio. On the other hand, however, the excitation spectra at 1 and 5 μM match for all the **DHNBDPs** within experimental uncertainty. The tendency to form the red-emitting species yet differs from dye to dye as exemplified by a comparison of **DHNBDP-H** and **DHNBDP-Me** in Figure S8.

In contrast to the behaviour of **BBDP-Ph** described in class (iv), the match of absorption and fluorescence excitation spectra in the **DHNBDP** series entirely rules out aggregate formation. Instead, the broadening of the spectra in water should be connected to a higher diversity of ground-state conformers which would be in accordance with our detailed investigation of ground-state conformers of dihydronaphthalene-appended BODIPYs published in Ref. [48]. The excited-state behaviour is dominated by two species, a rather resonantly emitting one and a strongly bathochromically emitting one. Such a behaviour can be ascribed to either an intramolecular charge transfer (CT) process such as twisted intramolecular charge transfer (TICT)[66] or the formation of excited dimers or excimers.[67] A differentiation between both processes is possible in a straightforward manner by studying the concentration-dependent behaviour: only in the case of the bimolecular excimer formation event should the band ratio depend on concentration. As Figures 10 and 11 impressively show, the bimolecular process indeed rules in the case of the **DHNBDP** dyes. Since excimer formation is rather efficient already at considerably low dye concentrations, we tentatively assume that a significant fraction of the dye monomers is sufficiently close in space, possibly forming loosely connected dimers which do not entail pronounced absorption spectroscopic shifts, for excitation to give rise to an excimer-type NIR fluorescence. Time-resolved fluorescence experiments support this assumption. Although three discrete decay components had to be employed for a global analysis of emission wavelength-resolved decays to yield acceptable fits with a global-χ^2 $\approx$1.0, the fast components of 8 ps (for **DHNBDP-H**), 31 ps (for **DHNBDP-Me**) and 48 ps (for **DHNBDP-Ph**) only dominates in the high-energy part of the spectrum as the major decay component. Species with intermediate lifetimes between 250 and 450 ps dominate in the wavelength range of 650–700 nm while slowly decaying species of 1.4–2.1 ns are found in the red region. Moreover, in the case of **DHNBDP-H** showing the most pronounced separation of short- and long-wavelength band, the fast decay component was found as a rise time at $>$750 nm. The occurrence of rise times hints at the fact that the fast decaying species that emits at shorter wavelengths populates the red emitting species only during the lifetime of the excited state.[46,68] According to excimer theory, a non-exponential decay of the monomer's fluorescence (in the blue region of the emission spectrum) hints at loosely bound excimers that already start to dissociate during the lifetime of the excited state.[69]

2.5.3. Class (vi): BODIPYs Forming Fluorescent Dimers

The last class of BODIPY dyes investigated here comprises the hydrophobic compounds **PBDP-Ph**, **PBDP-DMA** and **PBDP-CN** with two phenanthrene rings fused to the BODIPY core. Like for the **DHNBDPs**, the common feature of the **PBDPs** is a broad, structure-less and strongly red-shifted emission band in aqueous solution that is not observed in the organic solvent under the conditions used, except for **PBDP-DMA**, which however carries the dimethylanilino unit known to induce CT emission for BODIPYs in polar solvents.[23,46] For a more detailed mechanistic discussion of the CT photophysics of such systems, the reader is referred to the original publications.[46,49]

In general, the phenanthrene-appended **PBDP** derivatives show rather similar properties as the **DHNBDPs**. The absorption is considerably broadened in water, the shape persistent and independent of dye concentration (Figure 12), and a strong quenching of the emission in water is noticed. The **PBDP** dyes show a weak to moderate LE band and a red-shifted CT-like emission band; observation in both emission bands yields identical fluorescence excitation spectra, which perfectly match with the absorption spectra for all the dyes.

At first instance, the absence of a concentration dependence of the red-shifted emission suggests that CT state formation might be the dominant excited state process. However, the fact that the sequence of the electron-donating/accepting strength of the *meso*-substituents does not reflect the trend of the red-to-blue band ratio—phenyl $>$ dimethylanilino $>$ cyanophenyl, that none of the **PBDP** dyes shows a red-shifted broad band in a polar protic solvent such as

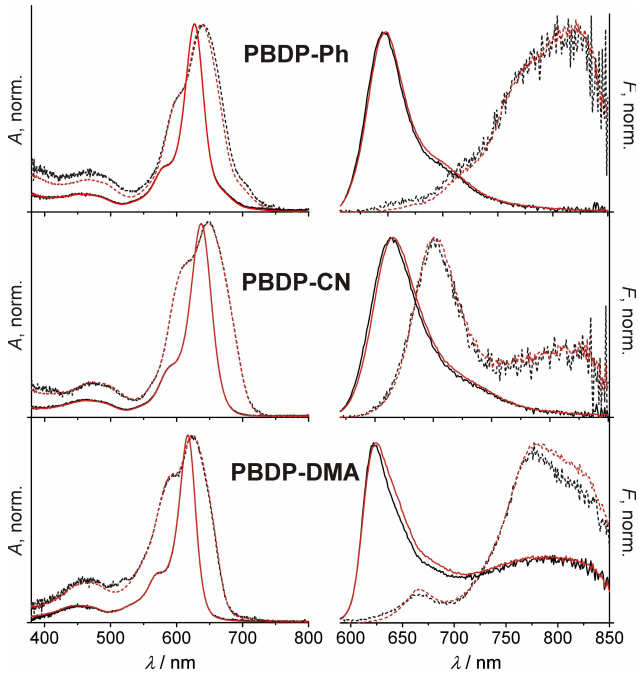

Figure 12. Normalized absorption and emission spectra of **PBDP-Ph**, **PBDP-CN** and **PBDP-DMA** in organic (solid lines) and aqueous solution (dotted lines) at 1 μM (black) and 5 μM (red) (λ_{ex} = 595 nm for **PBDP-Ph** and **PBDP-CN**; 570 nm for **PBDP-DMA**).

methanol (or only a very weak one in the case of **PBDP-DMA**),[49] and that the emission maximum of the red emission of **PBDP-DMA** occurs at almost the same position in water (801 nm, see Table 1) as in acetonitrile (798 nm, see Ref. [49]) does not support this assumption. Instead, it is again helpful to consider excimer theory. When pre-formed excimers are involved, i.e., when the two fluorophores form rather tightly bound dimers already in the ground state, excimer formation is so fast that the conventional kinetic signature of fast decay and rise times might not be observable with an instrument that can only resolve a few picoseconds like the one we had available.[69] Pre-formation of dimers is also supported by considering more closely the molecular structure of the three dyes in this series. **PBDP-Ph** with only planar aromatic entities in its structure can form the best aligned dimers. Considering electron deficiency/richness, **PBDP-DMA** with a *p*-dimethylamino group at the *meso*-phenyl substituent can then form better dimers than **PBDP-CN** with a cyanophenyl group. The lowest branch of Scheme 2 thus has to be rearranged (Scheme 3; Scheme S1).

3. Conclusions

BODIPY dyes that can be well dissolved in water commonly display identical or very similar spectroscopic properties in aqueous and organic media. These dyes would be very interesting for bio-labeling applications or chemical sensing in realistic media, since their optical properties would not depend significantly on the polarity, hydrophilicity or proticity features of the environment, rendering their optical response more reproducible. However, when screening the literature on BODIPY-based probes and labels it is apparent that most model studies are carried out in acetonitrile-water or alcohol-water[50,70] mixtures that utilize 30 vol.-% or more of the organic co-solvent, before frequently going even to more complex environments like cells without mentioning whether this step entails yet other changes in the dye's association chemistry, spectroscopic response or photophysical characteristics.[71–75] Our present study now indicates, for the first time, that such assumptions might well hold, for instance, for dyes such as **R_4BDP-H** or **BDP-Ph**,[76] yet that already subtle changes such as the introduction of a methyl group in the *meso*-position of the BODIPY core (**R_4BDP-Me** *vs.* **R_4BDP-H**) can influence the aggregation pattern of the dyes significantly and consequently, their optical properties.

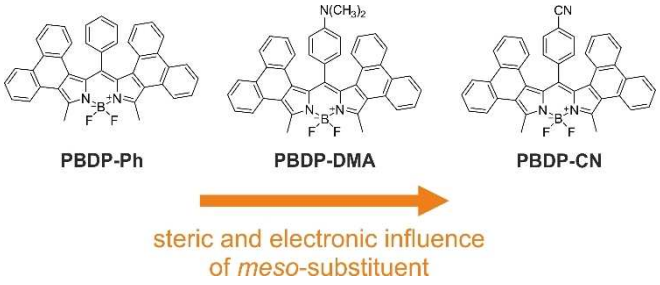

Scheme 3. Decisive modification sequence according to the extent of dimer formation in **PBDP** series.

In the case of **BDP-Ph**, the lack of methyl substituents in the BODIPY core allow for a better rotation of the *meso*-phenyl substituent, probably hindering dye aggregation in water and requiring higher concentrations to induce such features. **R_4BDP-Ph**, however, with two methyl groups in these positions displays a pronounced tendency for J aggregation in water. **R_2BDP-Ph**, which has methyl substituents in the 3- and 5-position shows a similar J aggregation, but only at higher concentration. In the case of **R_6BDP-Ph**, structurally very similar to **R_4BDP-Ph** the presence of two ethyl substituents at the 2- and 6-positions also seems to inhibit the formation of ordered spectroscopically active aggregates in water.

Fluorophores with aromatic π systems fused to the core do not seem to form aggregates in water, presumably because the steric strain of these highly crowded dyes does not allow for a close encounter and optimum alignment of several monomers for their electron systems to sufficiently couple. Moreover, whereas sterically rather rigid **BBDP-Ph** seems to exist in several ground-state species that do not interact in the excited state, the **DHNBDPs** and **PBDPs** show excited-state interaction features. For **DHNBDPs**, this leads to classical, concentration-dependent excimer formation, yet pre-formed dimers seem to govern the behaviour of the **PBDPs**, leading to an extraordinarily large Stokes shift of 170 nm especially in the case of **PBDP-Ph**.

Apparently, the spectroscopic features and photophysics of BODIPY dyes in water are rich. Since these studies were made in neat water, it is expected that association or excited-state reaction equilibria are qualitatively retained yet their magnitude will depend on electrolyte content, pH, type of buffer or other properties of real-world aqueous solutions. Figures S8 and S9 show representative results obtained for an initial screening of **DHNBDPs**, indicating a good qualitative agreement with the data in Figures 9–11. The diversity reported in this work impressively stresses the fact that BODIPYs do not only belong to the class of polymethine dyes and show their versatility and richness regarding aggregate formation, but that BODIPYs surpass traditional polymethines such as cyanine dyes because they also can be designed to show features of aromatic dyes like excimer formation. Excimer formation for instance might open the path for the design of functional dyes that operate according to this principle in an entirely new wavelength range, shifted for several hundred nanometers with respect to typical excimer dyes such as anthracene or pyrene.

Experimental Section

Synthesis

Compounds **R_6BDP-H**, **R_4BDP-Me**, **BDP-Ph** and **R_2BDP-Ph** were commercially available. **R_4BDP-H**, which is not commercially available anymore since several years, has been prepared by us according to a procedure reported in the literature.[77] **R_4BDP-H** was described in Ref. [46]. The aromatic ring-fused BODIPYs were prepared as described previously: **BBDP-Ph** as detailed in Ref. [47];

DHNBDP-H, **DHNBDP-Me** and **DHNBDP-Ph** were published in Ref. [48]; and the phenanthrene-fused BODIPYs **PBDP-Ph**, **PBDP-CN** and **PBDP-DMA** in Ref. [44].

Optical Spectroscopy

All solvents employed for the measurements were of spectroscopic grade and purchased from Aldrich. UV-Vis absorption spectra were recorded on an Analytik Jena Specord 210 Plus spectrophotometer. Steady-state fluorescence measurements were measured on Horiba Jobin-Yvon FluoroMax-4P and Spectronics Instrument 8100 spectrofluorometers, using standard 10 mm path length quartz cuvettes in a 90° standard geometry, with polarizers set at 54.7° for emission and 0° for excitation. For all measurements, the temperature was kept constant at 298 ± 1 K. Molar absorption coefficients were obtained from duplicate measurements of a single stock solution. All the emission spectra presented here were spectrally corrected as described in Ref. [78]; the excitation spectra are uncorrected. Fluorescence quantum yields in organic solvents were obtained with the comparative method as detailed in the Supporting Information. Φ_f in water could not been measured precisely due to the presence of species diversity in the ground state at the excitation wavelength. Moreover, the spectroscopic changes involving aggregation in water are transient, which makes fluorescence quantum yield determination of a defined species impossible.

Measurement solutions (1 μM and 5 μM) of the BODIPYs were prepared directly in the cuvette either in (i) 100% acetonitrile (as a reference of a neat organic medium) or in (ii) water with 2.5% (v/v) MeCN, by dilution of a ca. 0.2 mM stock solution of the corresponding dye dissolved in MeCN. The acetonitrile percentage in water was kept constant in all the experiments. Spectroscopic measurements have been carried out generally immediately after the solution preparation (< 5 min), except otherwise noted and for the time-dependent experiments.

Fluorescence lifetimes (τ_f) were determined by a unique customized laser impulse fluorometer with picosecond time resolution which was described earlier by us.[47] The fluorescence was collected at right angles (polarizer set at 54.7°; monochromator with spectral bandwidths of 4, 8, and 16 nm) and the fluorescence decays were recorded with a modular single photon timing unit. While realizing typical instrumental response functions of fwhm of ca. 25–30 ps, the time division was 4.8 ps channel^{-1} and the experimental accuracy amounted to ± 3 ps, respectively. The laser beam was attenuated using a double prism attenuator from LTB and typical excitation energies were in the nanowatt to microwatt range (average laser power). The fluorescence lifetime profiles were analysed with a PC using the software package Global Unlimited V2.2 (Laboratory for Fluorescence Dynamics, University of Illinois). The goodness of the fit of the single decays as judged by reduced chi-squared (χ_R^2) and the autocorrelation function C(j) of the residuals was always below $\chi_R^2 < 1.2$. Where indicated, several decays were recorded across the emission spectrum to allow for a global analysis of decays. Here, the decay times of the species were linked while the program varied the pre-exponential factors and lifetimes until the changes in the error surface (χ^2 surface) were minimal, that is, convergence was reached. The fitting results were judged for every single decay (local χ_R^2) and for all the decays (global χ_R^2), respectively. The errors for all the global analytical results presented here were below a global $\chi_R^2 = 1.2$.

Acknowledgements

This work was supported by the Spanish Ministry of Science and Innovation ("Ramón y Cajal" Program, grant for A.B.D.) and the Alexander von Humboldt Foundation (grants for A.B.D. and P.A.). We thank Katrin Hoffmann (BAM Div. 1.2) for help in obtaining CLSM images.

Conflict of Interest

The authors declare no conflict of interest.

Keywords: aggregates · BODIPY · excimers · fluorescence · photophysics

[1] A. Loudet, K. Burgess, *Chem. Rev.* **2007**, *107*, 4891–4932.
[2] G. Ulrich, R. Ziessel, A. Harriman, *Angew. Chem. Int. Ed.* **2008**, *47*, 1184–1201.
[3] A. B. Descalzo, H. J. Xu, Z. Shen, K. Rurack, *Ann. N. Y. Acad. Sci.* **2008**, *1130*, 164–171.
[4] N. Boens, V. Leen, W. Dehaen, *Chem. Soc. Rev.* **2012**, *41*, 1130–1172.
[5] A. Kamkaew, S. H. Lim, H. B. Lee, L. V. Kiew, L. Y. Chung, K. Burgess, *Chem. Soc. Rev.* **2013**, *42*, 77–88.
[6] Y. Ni, J. S. Wu, *Org. Biomol. Chem.* **2014**, *12*, 3774–3791.
[7] H. Lu, J. Mack, Y. C. Yang, Z. Shen, *Chem. Soc. Rev.* **2014**, *43*, 4778–4823.
[8] G. Fan, L. Yang, Z. J. Chen, *Front. Chem.* **2014**, *8*, 405–417.
[9] V. Lakshmi, M. R. Rao, M. Ravikanth, *Org. Biomol. Chem.* **2015**, *13*, 2501–2517.
[10] T. Kowada, H. Maeda, K. Kikuchi, *Chem. Soc. Rev.* **2015**, *44*, 4953–4972.
[11] N. Boens, B. Verbelen, W. Dehaen, *Eur. J. Org. Chem.* **2015**, 6577–6595.
[12] E. V. Antina, R. T. Kuznetsova, L. A. Antina, G. B. Guseva, N. A. Dudina, A. I. V'Yugin, A. V. Solomonov, *Dyes Pigm.* **2015**, *113*, 664–674.
[13] Y. Ge, D. F. O'Shea, *Chem. Soc. Rev.* **2016**, *45*, 3846–3864.
[14] H. Lu, J. Mack, T. Nyokong, N. Kobayashi, Z. Shen, *Coord. Chem. Rev.* **2016**, *318*, 1–15.
[15] H. Klfout, A. Stewart, M. Elkhalifa, H. S. He, *ACS Appl. Mater. Interfaces* **2017**, *9*, 39873–39889.
[16] S. Kolemen, E. U. Akkaya, *Coord. Chem. Rev.* **2018**, *354*, 121–134.
[17] L. Jean-Gerard, W. Vasseur, F. Scherninski, B. Andrioletti, *Chem. Commun.* **2018**, *54*, 12914–12929.
[18] L. Li, J. Han, B. Nguyen, K. Burgess, *J. Org. Chem.* **2008**, *73*, 1963–1970.
[19] S. L. Niu, G. Ulrich, R. Ziessel, A. Kiss, P.-Y. Renard, A. Romieu, *Org. Lett.* **2009**, *11*, 2049–2052.
[20] Y. Tokoro, A. Nagai, Y. Chujo, *Tetrahedron Lett.* **2010**, *51*, 3451–3454.
[21] S. L. Zhu, J. T. Zhang, G. Vegesna, F. T. Luo, S. A. Green, H. Y. Liu, *Org. Lett.* **2011**, *13*, 438–441.
[22] T. Bura, R. Ziessel, *Org. Lett.* **2011**, *13*, 3072–3075.
[23] S.-l. Niu, C. Massif, G. Ulrich, P.-Y. Renard, A. Romieu, R. Ziessel, *Chem. Eur. J.* **2012**, *18*, 7229–7242.
[24] A. Romieu, C. Massif, S. Rihn, G. Ulrich, R. Ziessel, P. Y. Renard, *New J. Chem.* **2013**, *37*, 1016–1027.
[25] T. T. Vu, M. Dvorko, E. Y. Schmidt, J. F. Audibert, P. Retailleau, B. A. Trofimov, R. B. Pansu, G. Clavier, R. Meallet-Renault, *J. Phys. Chem. C* **2013**, *117*, 5373–5385.
[26] N. K. Allampally, A. Florian, M. J. Mayoral, C. Rest, V. Stepanenko, G. Fernandez, *Chem. Eur. J.* **2014**, *20*, 10669–10678.
[27] L. Yang, G. Fan, X. K. Ren, L. Y. Zhao, J. K. Wang, Z. J. Chen, *Phys. Chem. Chem. Phys.* **2015**, *17*, 9167–9172.
[28] A. Rodle, M. Lambov, C. Muck-Lichtenfeld, V. Stepanenko, G. Fernandez, *Polymer* **2017**, *128*, 317–324.
[29] The Molecular Probes® Handbook, 11th Ed., Thermo Fisher Scientific: https://www.thermofisher.com/de/de/home/references/molecular-probes-the-handbook/fluorophores-and-their-amine-reactive-derivatives/bodipy-dye-series.html#datatable (accessed May 2019).
[30] Search topics: (DYE* or FLUOROPHOR* or CHROMOPHOR* or LABEL* or PROBE* or SENSOR* or STAIN* or CHEMOSENSOR* or INDICATOR*) and RHODAMIN* or FLUORESCEIN* or CYANIN* or (BODIPY* or borondipyr-

romethen* or boron-dipyrrin*); for total dyes: (DYE* or FLUOROPHOR* or CHROMOPHOR* or STAIN*)
[31] Y. Ni, L. T. Zeng, N. Y. Kang, K. W. Huang, L. Wang, Z. B. Zeng, Y. T. Chang, J. S. Wu, *Chem. Eur. J.* **2014**, *20*, 2301–2310.
[32] C. Massif, S. Dautrey, A. Haefele, R. Ziessel, P.-Y. Renard, A. Romieu, *Org. Biomol. Chem.* **2012**, *10*, 4330–4336.
[33] K. M. Bardon, S. Selfridge, D. S. Adams, R. A. Minns, R. Pawle, T. C. Adams, L. Takiff, *ACS Omega* **2018**, *3*, 13195–13199.
[34] J. Xu, Q. Li, Y. Yue, Y. Guo, S. Shao, *Biosens. Bioelectron.* **2014**, *56*, 58–63.
[35] J. Isaad, A. El Achari, *Analyst* **2013**, *138*, 3809–3819.
[36] M. R. Martinez-Gonzalez, A. Urias-Benavides, E. Alvarado-Martinez, J. C. Lopez, A. M. Gomez, M. del Rio, I. Garcia, A. Costela, J. Banuelos, T. Arbeloa, I. Lopez Arbeloa, E. Pena-Cabrera, *Eur. J. Org. Chem.* **2014**, *2014*, 5659–5663.
[37] M. M. Kose, S. Onbulak, I. I. Yilmaz, A. Sanyal, *Macromolecules* **2011**, *44*, 2707–2714.
[38] S. K. Yang, X. Shi, S. Park, T. Ha, S. C. Zimmerman, *Nat. Chem.* **2013**, *5*, 692–697.
[39] B. Sui, S. Tang, A. W. Woodward, B. Kim, K. D. Belfield, *Eur. J. Org. Chem.* **2016**, *2016*, 2851–2857.
[40] S. L. Niu, C. Massif, G. Ulrich, R. Ziessel, P.-Y. Renard, A. Romieu, *Org. Biomol. Chem.* **2011**, *9*, 66–69.
[41] M. Collot, E. Boutant, M. Lehmann, A. S. Klymchenko, *Bioconjugate Chem.* **2019**, *30*, 192–199.
[42] S. Atilgan, T. Ozdemir, E. U. Akkaya, *Org. Lett.* **2008**, *10*, 4065–4067.
[43] M. Tasior, J. Murtagh, D. O. Frimannsson, S. O. McDonnell, D. F. O'Shea, *Org. Biomol. Chem.* **2010**, *8*, 522–525.
[44] A. B. Descalzo, H. J. Xu, Z. L. Xue, K. Hoffmann, Z. Shen, M. G. Weller, X. Z. You, K. Rurack, *Org. Lett.* **2008**, *10*, 1581–1584.
[45] M. Baglan, S. Ozturk, B. Gur, K. Meral, U. Bozkaya, O. A. Bozdemir, S. Atilgan, *RSC Adv.* **2013**, *3*, 15866–15874.
[46] M. Kollmannsberger, K. Rurack, U. Resch-Genger, J. Daub, *J. Phys. Chem. A* **1998**, *102*, 10211–10220.
[47] Z. Shen, H. Rohr, K. Rurack, H. Uno, M. Spieles, B. Schulz, G. Reck, N. Ono, *Chem. Eur. J.* **2004**, *10*, 4853–4871.
[48] Y. W. Wang, A. B. Descalzo, Z. Shen, X. Z. You, K. Rurack, *Chem. Eur. J.* **2010**, *16*, 2887–2903.
[49] A. B. Descalzo, H. J. Xu, Z. Shen, K. Rurack, *J. Photochem. Photobiol. A* **2018**, *352*, 98–105.
[50] M. Hecht, W. Kraus, K. Rurack, *Analyst* **2013**, *138*, 325–332.
[51] E. Climent, M. Hecht, H. Witthuhn, K. Gawlitza, K. Rurack, *ChemistryOpen* **2018**, *7*, 957–968.
[52] F. Bergstrom, I. Mikhalyov, P. Hagglof, R. Wortmann, T. Ny, L. B. A. Johansson, *J. Am. Chem. Soc.* **2002**, *124*, 196–204.
[53] I. Mikhalyov, N. Gretskaya, F. Bergstrom, L. B. A. Johansson, *Phys. Chem. Chem. Phys.* **2002**, *4*, 5663–5670.
[54] D. Tleugabulova, Z. Zhang, J. D. Brennan, *J. Phys. Chem. B* **2002**, *106*, 13133–13138.
[55] M. A. H. Alamiry, A. C. Benniston, G. Copley, A. Harriman, D. Howgego, *J. Phys. Chem. A* **2011**, *115*, 12111–12119.
[56] A. C. Benniston, G. Copley, A. Harriman, D. Howgego, R. W. Harrington, W. Clegg, *J. Org. Chem.* **2010**, *75*, 2018–2027.
[57] R. E. Pagano, O. C. Martin, H. C. Kang, R. P. Haugland, *J. Cell Biol.* **1991**, *113*, 1267–1279.
[58] G. M. Makrigiorgos, *J. Biochem. Biophys. Methods* **1997**, *35*, 23–35.
[59] A. J. Musser, S. K. Rajendran, K. Georgiou, L. Gai, R. T. Grant, Z. Shen, M. Cavazzini, A. Ruseckas, G. A. Turnbull, I. D. W. Samuel, J. Clark, D. G. Lidzey, *J. Mater. Chem. C* **2017**, *5*, 8380–8389.
[60] J. H. Olivier, J. Widmaier, R. Ziessel, *Chem. Eur. J.* **2011**, *17*, 11709–11714.
[61] F. R. Li, S. I. Yang, Y. Z. Ciringh, J. Seth, C. H. Martin, D. L. Singh, D. H. Kim, R. R. Birge, D. F. Bocian, D. Holten, J. S. Lindsey, *J. Am. Chem. Soc.* **1998**, *120*, 10001–10017.
[62] Confocal laser scanning microscopy (CLSM) images of the first three groups of dyes were recorded by evaporation under the microscope. Whereas **R_4BDP-H** produces neat images without the formation of any particulate objects, **R_4BDP-Me** and **R_4BDP-Ph** show the formation of particles of few hundred nanometer sizes.
[63] M. van Burgel, D. A. Wiersma, K. Duppen, *J. Chem. Phys.* **1995**, *102*, 20–33.
[64] S. Kirstein, S. Dähne, *Int. J. Photoenergy* **2006**, *2006*, Article ID 20363.
[65] L. J. Patalag, L. P. Ho, P. G. Jones, D. B. Werz, *J. Am. Chem. Soc.* **2017**, *139*, 15104–15113.
[66] W. Rettig, *Top. Curr. Chem.* **1994**, *169*, 253–299.
[67] P. K. Misra, P. Somasundaran, *Adv. Polym. Sci.* **2008**, *218*, 143–188.
[68] Although it is rather unlikely that the excited state deactivation mechanism involves three distinct species in a consecutive reaction sequence, this is the best possible model to be employed here because a fit invoking for instance lifetime distributions, which would more closely describe a heterogeneous ensemble like the present one, would not yield reliable rise times.
[69] B. Valeur, in *Molecular Fluorescence: Principles and Applications*, Wiley-VCH, Weinheim, **2001**, pp. 94–99.
[70] The behaviour of BODIPYs in alcohol–water mixtures is very similar to that in acetonitrile–water and fractions of the organic solvent of $>40\%$ are required for unaltered performance.
[71] X. J. Peng, J. J. Du, J. L. Fan, J. Y. Wang, Y. K. Wu, J. Z. Zhao, S. G. Sun, T. Xu, *J. Am. Chem. Soc.* **2007**, *129*, 1500–1501.
[72] M. J. Yuan, Y. L. Li, J. B. Li, C. H. Li, X. F. Liu, J. Lv, J. L. Xu, H. B. Liu, S. Wang, D. Zhu, *Org. Lett.* **2007**, *9*, 2313–2316.
[73] Q. Li, Y. Guo, S. J. Shao, *Analyst* **2012**, *137*, 4497–4501.
[74] M. Pamuk, F. Algi, *Tetrahedron Lett.* **2012**, *53*, 7010–7012.
[75] K. Liu, X. J. Zhao, Q. X. Liu, J. Z. Huo, Z. C. Li, X. X. Wang, *Sens. Actuators B* **2017**, *239*, 883–889.
[76] It shall be noted however that it has been proven especially for **LBDP1** and **R_4BDP-H**, "innocent dyes" in terms of our present investigations in molecular form in neat water, that the behaviour can change dramatically in the presence of biomolecular environments, see section on PREVIOUS OBSERVATIONS ON ASSOCIATION.
[77] L. X. Wu, K. Burgess, *Chem. Commun.* **2008**, 4933–4935.
[78] U. Resch-Genger, D. Pfeifer, C. Monte, W. Pilz, A. Hoffmann, M. Spieles, K. Rurack, J. Hollandt, D. Taubert, B. Schonenberger, P. Nording, *J. Fluoresc.* **2005**, *15*, 315–336.

Manuscript received: September 30, 2019
Accepted manuscript online: October 8, 2019
Version of record online: October 29, 2019